Onset and forecast of the 1994-1995 El Niño event: equatorial Rossby wave reflection evidenced by TOPEX/POSEIDON

Boulanger, J.-P., L.-L. Fu and C. Perigaud

Jet Propulsion Laboratory/California Institute of Technology

MS 300-323

4800 Oak Grove Drive

Pasadena, CA 91109, USA.

We found evidence in TOPEX/POSEIDON sea level data that equatorial first meridional mode Rossby waves reflected at the Pacific western boundary into Kelvin waves during the January-July 1994 period prior to the 1994-1995 El Niño event. By analyzing data and using a simple coupled ocean-atmosphere model, we demonstrated that this reflection was a key mechanism for the onset of the 1994-1995 El Niño event.

Long equatorial waves[1,2] in the Pacific ocean have been suggested to play a major role in the El Niño/Southern Oscillation (ENSO) events through a mechanism commonly referred to as the delayed action oscillator mechanism[3,4]. These waves are Kelvin waves propagating eastward at a speed close to 2.5-3 .0m/s, and Rossby waves propagating westward (the first-mode Rossby wave travels at about 1.Om/s to the west). They are affected by wind forcing (mainly the zonal wind stress) as well as by reflection at the equatorial Pacific maritime boundaries. In particular, the reflection of first-mode Rossby waves at the Pacific western boundary into eastward-propagating Kelvin waves is critical for sustaining the ENSO-like variability suggested by the delayed action oscillator mechanism[4]. While Kelvin and Rossb y waves have been observed in data[5,6] and, especially, in altimetric data from the GEOSAT[7] and TOPEX/POSEIDON[8,9] missions, no evidence has been given for the reflection of Rossby waves at the western boundary to play a significant role in the onset of an ENSO event. Here, we first present how TOPEX/POSEIDON sea level data allows to observe long Rossby wave reflection at the Pacific western boundary. Then, using the Zebiak and Cane[10] model improved by Dcwitte and Perigaud[11], wc show that this reflection initiated the El NIño event observed in the tropical Pacific in late 1994-early 1995.

The TOPEX/POSEIDON (T/P hercfater) sca level data[12] from November 1992 to January 1995 presented in Boulanger and Fu (manuscript submitted) were used in this study. Briefly, along-track data were binned into a 3“ longitude by 0.5° latitude grid every 10 days and filtered with a 50-day Harming filter. Sea level anomalies were computed relative to the mean calculated over the 1993-1994 period, Kelvin and first-mode Rossby wave coefficients were calculated from T/P sea level data using the decomposition method developped by Boulanger and Menkes[9]. This method basically calculates the projection of the sea level data onto the meridional structures of the waves, resulting in wave coefficients as functions of longitude and time. The evidence of the wave

propagation asshown in Figures 1a-b validates *a posteriori* the decomposition method. Figure 1a displays the first meridional mode Rossby wave coefficient from 80"W to 130"E with east pointing to the left as opposed to Figure lb where the Kelvin wave coefficient is displayed from 130°E to 80°W. This representation of wave coefficients allows to depict potential reflection of Rossby waves into Kelvin waves at the western boundary (130°E). Boulanger and Fu (manuscript submitted) have shown that most of the Kelvin wave signals east of 165°E can be explained by the wind variability. However, west of 165"E, a large variance of the signal is not explained by the wind forcing. We will show that, at least, from January to July 1994, the signal is explained by the reflection of long Rossby waves at the western boundary.

At the western boundary, the January-July 1994 period was the only time when the impinging Rossby waves and the eastward-propagating Kelvin waves displayed coherent amplitude and phase. To investigate this potential relationship, wc present time series of the two coefficients at 144"E (Figure 2) where the Rossby coefficient time series is shifted by 30 days to account for the time of wave propagation to the boundary and back assuming a 2.5m/s baroclinic phase speed, The two time series show a fairly good agreement in phase during the January-July 1994. Moreover the ratio of amplitudes of the Rossby and Kelvin coefficients during this period is compatible with the theory (Boulanger and Fu, manuscript submitted). This result confirms the relationship observed in Figures 1 a and 1 b between the two coefficients at the wcstem boundary. Therefore, thanks to the high accuracy of the TOPEX/POSEIDON data, reflection of long Rossby waves at the Pacific western boundary is clearly observed. Two major questions then arise: 1/ why is reflection observed only during the January-July 1994 period?, 2/ did the reflection play a role in the onset of the warm conditions observed in late 1994? In the following, we will focus on this second question.

Observed conditions in 1994 were analyzed using T/P sea level (presented above), sea surface temperature (SST)[13], and ERS-1 zonal wind stress data (courtesy of Dr. T. Liu [14]). Both SST and wind stress data (Figure 3) are anomalies relative to the mean computed over the 1993-1994 period. In December 1993, strong easterly wind anomalies (negative values) were observed from 160"E to 110°W (Figure 3b). The effect of these wind anomalies, together with the propagation from the eastern boundary of a downwelling Rossby wave (Figure la) advecting cold waters from the east to the west, contributed to the development of negative SST anomalies in the central Pacific. These SST anomalies decreased in amplitude in early 1994 but remained negative near the dateline until June-July 1994 when they reversed to positive anomalies.

We thus believe that the following mechanism involving long wave propagation and reflection was at work during the first half of 1994. In responses to the negative SST anomalies near the dateline (Figure 3a), easterly wind anomalies (Figure 3b) were induced west of the dateline. These wind anomalies forced upwelling Kelvin waves (Figure lb) which propagated toward the eastern Pacific and downwelling Rossby waves (Figure la) which travelled to the western boundary and reflected there as downwelling Kelvin waves (Figures 1 and 2). The downwelling Kelvin signal propagated eastward but could not pass the dateline as it was cancelled by the upwelling Kelvin signal generated by the easterly anomalies. Neverthless, they eroded the negative SST anomalies located near the dateline by advecting warm waters from the west and deepening the thermocline (the SST anomalies indeed decreased during March-May) and acted to weaken and eventuall y reverse the negative anomalies to positive in June 1994. Simultaneously, the easterly wind anomalies weakened and eventually reversed to weak westerly wind anomalies. The wind reversal only partially explained the strong downwelling Kelvin wave observed in July propagating throughout the entire basin from the western boundary (Boulanger and Fu, manuscript submitted). The warm SST anomalies near the dateline

were then favorable to the development of convection and warmer conditions observed in late 1994 and early 199514.

To demonstrate this scenario, wc used a simple coupled ocean-atmosphere model in which the ocean has one vertical dynamic mode with an embedded mixed layer of constant depth, and the atmosphere is one layer driven by the SST anomaly field. The equations and parameters are described in Zebiak and Cane[10]. The parametrization of the subsurface temperature in the ocean and that of the heat released by moisture convection in the atmosphere were based on Dewitte and Perigaud[11]. It is worth noting that the model computes outputs relative to the climatology prescribed in Zebiak and Cane[10]. The difference in the reference fields is a source of discrepancy between the observed anomalies (referenced to the 1993-1994 mean) shown in Figures 1 or 3 and the simulated ones (referenced to a prescribed climatology) shown hereafter. However, this is not an impediment for our study as we are interested in a qualitative investigation of the mechanism responsible for the reversal of the conditions in the central Pacific in June-July 1994. Initial conditions for the coupled simulations were defined as follows: first, the T/P sea level anomalies from October 1992 to January 1995 were referenced to the climatology derived from hydrographic data and projected on Kelvin and Rossby waves; second, these wave components were assimilated in the ocean and the atmosphere models in order to compute a series of conditions available for initiating the coupled model for forecasts. The experiments examined here arc 12-month long coupled model runs starting from the initial conditions of December 1993. We did three different forecast experiments. For each of them, equatorial zonal wind stress (ZWSA), sca surface temperature (SSTA) and sea level (SLA) monthly interannual anomalies arc plotted.

In the first experiment (Figures 4a-c), the Kelvin wave coefficient at the western boundary was defined as in Zebiak and Cane[10]: the zonal current (a sum of Rossby and Kelvin wave contributions) integrated over the western boundary is equal to zero. From

January to May 1994, SSTA were negative over most of the basin. The maximum negative values located near 160”E were slightly displaced westward as they decreased in amplitude. Simultaneously, ZWSA were easterlies west of the maximum negative SSTA. The amplitude of the easterlies near the dateline were displaced westward and decreased in amplitude until July when they eventually reversed. In agreement with the mechanism suggested above, a strong downwelling sea level anomalies were simulated west of the dateline, and this signal was later covering the entire basin in June-July 1994. Therefore the coupled model simulated an event coherent in phase (at least during the first half of 1994) with the observations. To investigate the role of the western boundary in the development of the conditions near the dateline in 1994, in a second experiment (Figures 4d-f), the Kelvin coefficient was set to zero at the western boundary: the Rossby wave signal impinging at the western boundary was not allowed to reflect. The first four months of the simulation are similar to those of the first experiment. However, no downwelling signal was observed throughout the basin in mid-1994, ZWSA and SSTA decreased until June. Beyond, they intensified, and the simulation evolved into a cold phase, These two first experiments showed that the reflection of Rossby waves at the western boundary were fundamental for the reversal of the conditions in June-July 1994. To investigate if the first meridional mode Rossby wave contribution was sufficient to explain the Kelvin wave amplitude and to allow the reversal as suggested by the data, wc did a third experiment (Figures 4g-i) where the baroclinic signal at the western boundary was projected onto long Rossby waves, and only the first meridional mode Rossby wave was allowed to contribute to the reflected Kelvin wave amplitude. The coupled model evolved as the first experiment. There is only a small difference in the timing of the reversal. The similarity between the first and third experiments shows the dominant role of the first-mode Rossby waves in the reflected Kelvin wave amplitude during the first half of 1994 as observed earlier in the T/P sea level data (Figures1 and 2).

These experiments have clearly indicated the critical role played by the reflection of the first-mode Rossby waves into Kelvin waves in the onset of an ENSO event. Without the reflection, the negative SST anomalies were not able to reverse into positive anomalies in June-July 1994 in the central Pacific. Without the positive SST anomalies, the easterly wind anomalies were not able to reverse into westerly anomalies after June-July, which were ultimately responsible for the 1994-1995 warming[14]. The reflection of first-mode Rossby waves into Kelvin waves at the western boundary from January to July 1994 was therefore a key mechanism for the onset of the 1994-1995 El Niño event observed in the equatorial Pacific ocean. Further investigation is needed to understand why the reflection of Rossby waves was observed only in January-July 1994. There is no doubt that longer time series of altimetric data will help considerably in detecting such processes and in providing a better understanding of the mechanisms responsible for the short-term climate variability in the tropical Pacific.

Acknowledgements.

The research described in this paper was carried out by the Jet Propulsion Laboratory, California Institue of Technology, under contract with National Aeronautics , and Space Administration, The authors want to thank Greg Pihos, Akiko Hayashi for their assistance with processing the TOPEX/POSEIDON data, as well as Tim Liu for his provision of the ERS-1 scaterrometer data. Support from the TOPEX/POSEIDON Project and the NSCAT Project is acknowledged.

References

1. Cane, M. A., and E. Sarachik, Forced baroclinic ocean motions, I: The linear equatorial unbounded case, *J. Mar. Res.*, 34,629-665, 1976.

2. Moore, D. W., and S. G. H. Philander, Modeling of the tropical oceanic circulation, The*sea,* 6,319-361, 1977.

3. Schopf, P. S., and M. J. Suarez, Vacillations in a coupled ocean-atmosphere model, *J. Atmos. Sci. ,45,549-566,* 1988.

4. Battisti D. S., Dynamics and thermodynamics of a warming event in a coupled tropical atmosphere-ocean model, *J. Atmos. Sc.*, 45,2889-2819, 1988.

5. Knox, R. A., and D. Halpern, Long range Kelvin wave propagation of transport variations in Pacific Ocean equatorial currents, *J. Mar. Res.,* 40, Suppl., 329-339, 1982.

6. Lukas, R., and E. Firing, The annual Rossby wave in the central equatorial Pacific Ocean, *J. Phys. Oceanogr., 15,55-67,* 1985.

7. Delcroix, T., J.-P. Boulanger, F. Masia, and C. Menkes, GEOSAT-derived sea level and surface-current anomalies in the equatorial Pacific, during the 1986-1989 El Niño and La Niña, *J. Geophys. Res., 99,25093-25107, 1994.*

8. Busalacchi, A. J., M. J. McPhadcn, and J. Picaut, Variability in equatorial Pacific sea surface topography during the verification phase of the TOPEX/POSEIDON Mission, J. Geophys. Res., 99,25,725-25,738, 1994.

9. Boulanger, J.-P, and C. Menkes, Propagation and reflection of long equatorial waves in the Pacific ocean during the 1992-1993 El Niño, *J. Geophys. Res.,* December 1995.

10. Zebiak, S. E., and M. A. Cane, A model El Niiio-Southern Oscillation, *Mon. Wea. Rev., 115,2262-2278, 1987.*

11. Dewitte, B., and C. Perigaud, El Niño-La Niña events with Cane and Zebiak's model and observed with satellite or in situ data. Part 2: model forced with observations, *J.* Climate, in press.

12. Fu, L.-L., E. J. Christensen, C. Yamarone, M. Lefebvre, Y. Menard, M. Dorrer, and P. Escudier, TOPEX/POSEIDON mission overview, *J. Geophys. Res.*, *99,24369-24381.*

13. Reynolds, R. W., A real-time global sea surface temperature analysis, *J. Climate*, **1,75-86,** 1988.

14. Liu, W. T., W. Tang, and L.-L. Fu, Recent warming event in the Pacific may bean ElNiño, EOS, 76,43, 1995.

15. Gill, A. E., Some simple solutions for the heat-induced tropical circulation, Q, *J. R. Meteor. Sot.,* **106,447-462,** 1980.

Figures

Figure 1: Longitude time plots of (a: left) the first-mode Rossby wave coefficient from 80°W to 130°E, and (b: right) the Kelvin wave coefficient from 130"E to 80°W. Coefficients are calculated from TOPEX/POSEIDON sea level data. They are non- dimensionnalised. Contour intervals are every 10 units. Positive values are shaded. An oceanic coefficient of 10 units would yielcd to a sea level amplitude of 3.2 cm for the Kelvin wave at the equator, and 2.8 cm for the Rossby wave at 4"N.

Figure 2: Time series at 144°E of the Kelvin coefficient (solid line) and the first-mode Rossby coefficient lagged by a 30-day period (da.shed line).

Figure 3: (a: left) Equatorial section of sea surface temperature anomalies (anomalies are relative to the January 1993 -Dccembcr 1994 two-year mean; contour intervals are every O. S"C); (b: right) Equatorial section of ERS- 1 zonal wind stress anomalies (contour intervals are every 0.1 $dyn.cm^{-2}$; a negative anomaly denotes an easterly wind anomaly). Positive anomalies are shaded.

Figure 4: Forecasts for the three experiments of (left) zonal wind stress interannual anomalies (ZWSA; contour intervals are every 0.05 $dyn.cm^{-2}$), (center) sea surface temperature interannual anomalies (SSTA; contour intervals are every 0.25°C), (right) sea level interannual anomalies (SLA; contour intervals are every 2cm). In the first experience, all the Rossby signal contributed to the Kelvin amplitude at the western boundary. In the second experiment, no Rossby signal was allowed to reflect into the Kelvin wave at the western boundary. In the third experiment, only the first meridional mode Rossby wave contributed to the Kelvin wave amplitude at the western boundary. In each plot, positive anomalies are shaded

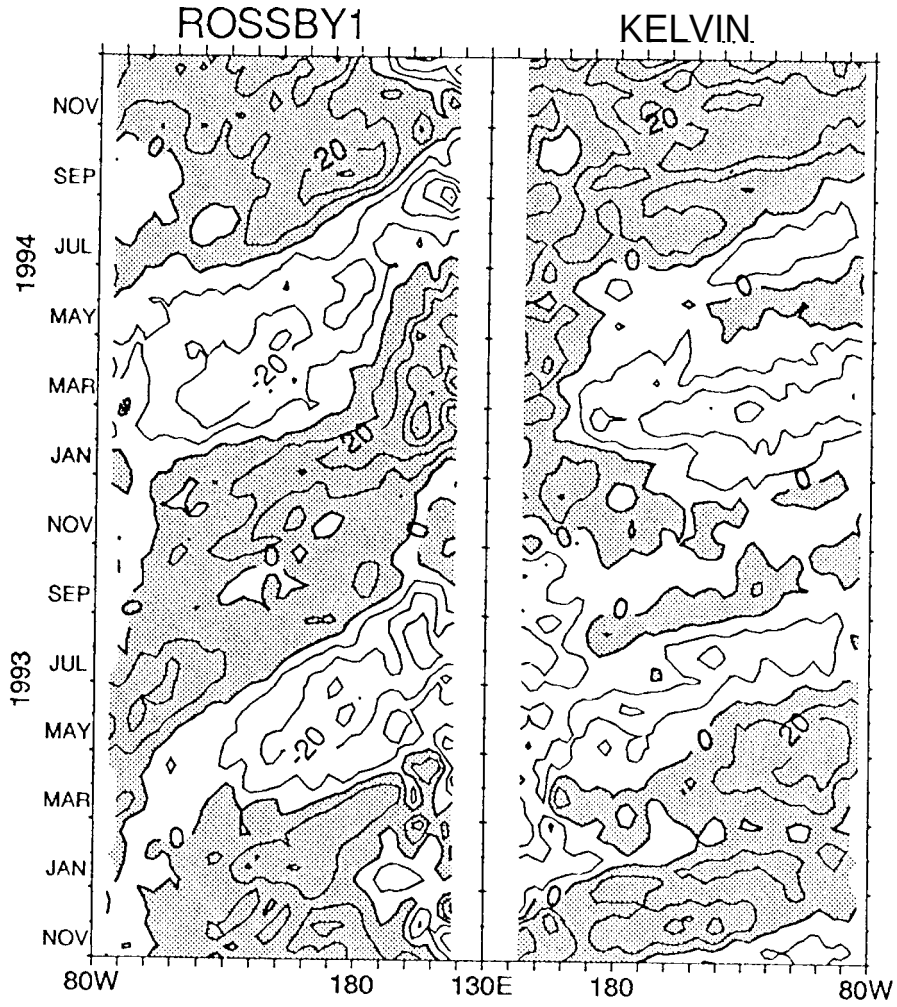
ROSSBY1
KELVIN
NOV
SEP
JUL
MAY
MAR
JAN
NOV
SEP
JUL
MAY
MAR
JAN
NOV
1994
1993
20
0
-20
80W
180
130E
180
80W

Fig. 1

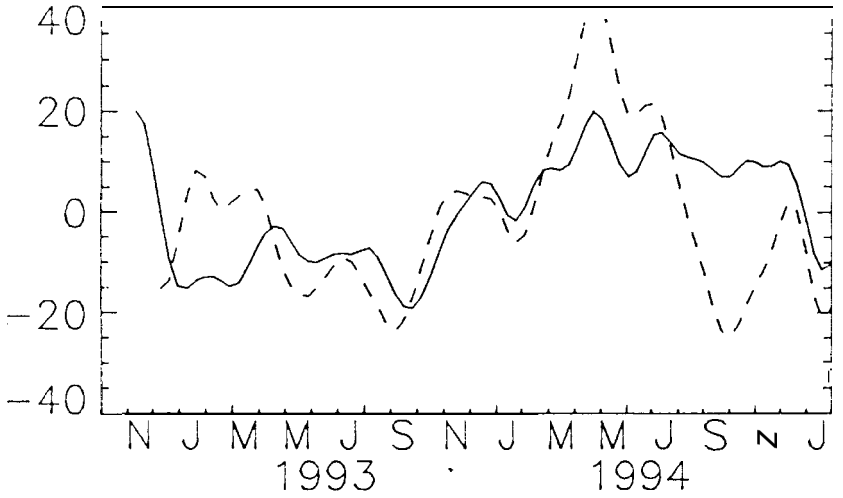

Fig 2

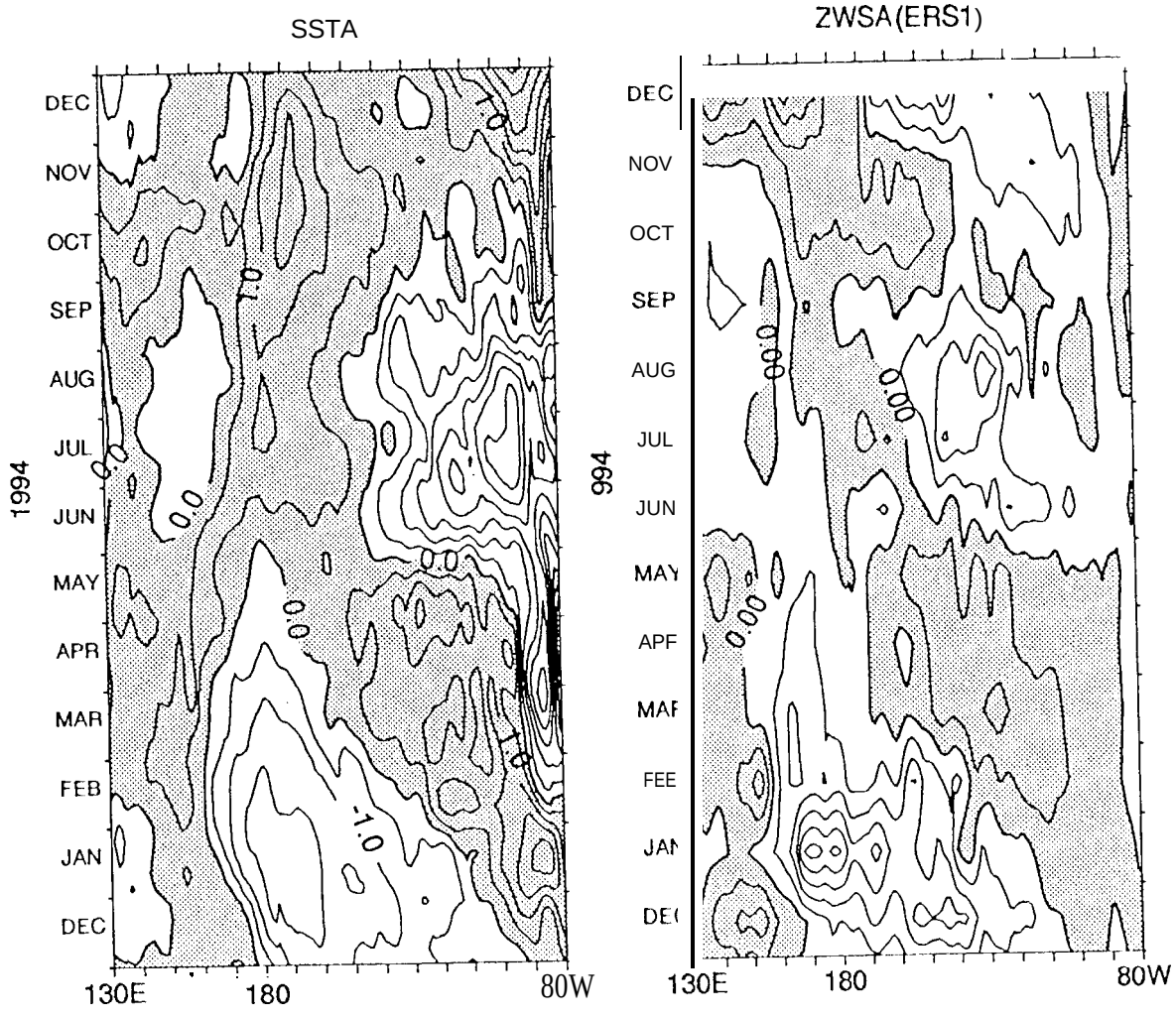
SSTA
ZWSA(ERS1)
1994
994
DEC
NOV
OCT
SEP
AUG
JUL
JUN
MAY
APR
MAR
FEB
JAN
DEC
130E
180
80W
0.0
-1.0
0.00

Fig. 3

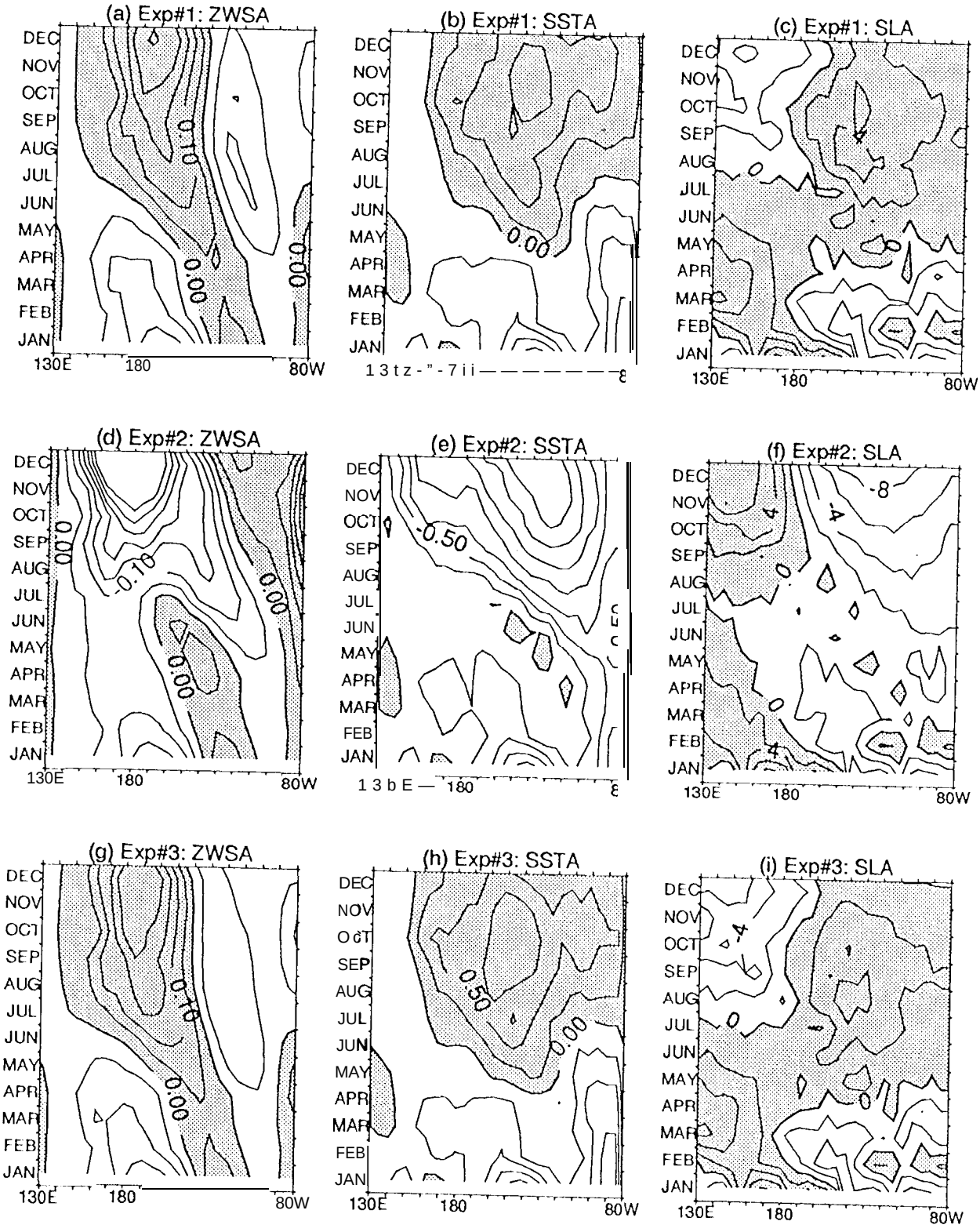
(a) Exp#1: ZWSA
(b) Exp#1: SSTA
(c) Exp#1: SLA
(d) Exp#2: ZWSA
(e) Exp#2: SSTA
(f) Exp#2: SLA
(g) Exp#3: ZWSA
(h) Exp#3: SSTA
(i) Exp#3: SLA
DEC
NOV
OCT
SEP
AUG
JUL
JUN
MAY
APR
MAR
FEB
JAN
130E
180
80W

Fig. 4